LOOPS AND LOOP CLOUDS – A NUMERICAL APPROACH TO THE WORLDLINE FORMALISM IN QED –*

Holger Gies
CERN, Theory Division
CH-1211 Geneva 23, Switzerland

Kurt Langfeld
Institut für theoretische Physik, Universität Tübingen
D-72076 Tübingen, Germany

A numerical technique for calculating effective actions of electromagnetic backgrounds is proposed, which is based on the string-inspired worldline formalism. As examples, we consider scalar electrodynamics in three and four dimensions to one-loop order. Beyond the constant-magnetic-field case, we analyze a step-function-like magnetic field exhibiting a nonlocal and nonperturbative phenomenon: "magnetic-field diffusion". Finally, generalizations to fermionic loops and systems at finite temperature are discussed.

1. Introduction

The computation of effective energies and effective actions of a quantum system is a general and frequently occurring problem in quantum field theory. In a given classical background, virtual quantum processes such as vacuum polarization modify the properties of the vacuum and are responsible for new nonlinear and nonlocal phenomena. These phenomena can often be described by an effective action that takes the virtual quantum processes into account. A prominent example is given by the Heisenberg-Euler action[1,2], describing the nonlinear corrections to the Maxwell action which are induced by virtual loops of electrons and positrons.

The Heisenberg-Euler action is the one-loop QED effective action,

$$\Gamma_{\rm eff}^{\rm spinor} = \ln\det(-{\rm i}\partial\!\!\!/ + A\!\!\!/ - {\rm i}m), \quad \Gamma_{\rm eff}^{\rm scalar} = -\ln\det(-(\partial + {\rm i}A)^2 + m^2), \qquad (1)$$

(here in Euclidean formulation), evaluated for a constant electromagnetic background field, and thereby represents a valid approximation of low-energy QED for all backgrounds that vary slowly with respect to the Compton wavelength $1/m$.

Technical difficulties increase markedly if one wants to go beyond this approximation. The standard means is the derivative expansion[3]; its application is however limited to backgrounds whose spacetime variation does not exceed the scale of the electron mass or the scale of the field strength. Moreover, the enormous proliferation of terms restricts the actual computations to low orders. Only for very special (and very rare) field configurations can the derivative expansion be summed up[4]. Numerical methods developed so far aim at the integration of the corresponding differential equation of the operators in Eq. (1); therefore, they have been applied only

*Talk given by H. Gies at the *Fifth Workshop on Quantum Field Theory under the Influence of External Conditions*, Leipzig, Germany, September, 2001.

to highly symmetric background fields up to now[5]. Of course, also the brute force method of spacetime discretization (lattice) can be employed, which has its own shortcomings (finite-size problems, fermion doubling, problems with many scales).

In this note, we advocate a recently developed numerical technique[6] which is based on the string-inspired worldline formalism[7] applied to QED with background fields[8]. The idea of the approach consists of rewriting the functional determinants contained in Eq. (1) in terms of 1-dim. path integrals, which finally can be evaluated with Monte-Carlo techniques. In contrast to the techniques mentioned above, our worldline numerics makes no reference to the particular properties of the background field and is therefore applicable to a wide class of configurations. In the following, we describe the approach in more detail and list a number of examples of a basic nature.

2. Basics of worldline numerics

In the following, we first concentrate on scalar QED, starting with the unrenormalized, but regularized Euclidean one-loop effective action in D dimensions in worldline representation[9], corresponding to the second equation of (1),

$$\Gamma_{\rm eff}^{\rm scalar}[A] = \int\limits_{1/\Lambda^2}^{\infty} \frac{dT}{T}\, {\rm e}^{-m^2 T}\, \mathcal{N} \int\limits_{x(T)=x(0)} \mathcal{D}x(\tau)\, {\rm e}^{-\int_0^T d\tau \left(\frac{\dot{x}^2}{4} + {\rm i}e\, \dot{x}\cdot A(x(\tau))\right)}. \qquad (2)$$

Here we encounter a path integral over closed loops in spacetime. Note that there are no other constraints to the loops except differentiability and closure; in particular, they can be arbitrarily self-intersecting and knotty. Introducing the Wilson loop

$$W[A(x)] = {\rm e}^{-{\rm i}e\int_0^T d\tau\, \dot{x}(\tau)\cdot A(x(\tau))} \equiv {\rm e}^{-{\rm i}e\oint dx\cdot A(x)}, \qquad (3)$$

Eq. (2) can be rewritten in a compact form:

$$\Gamma_{\rm eff}^{\rm scalar}[A] = \frac{1}{(4\pi)^{D/2}} \int d^D x_0 \int\limits_{1/\Lambda^2}^{\infty} \frac{dT}{T^{(D/2)+1}}\, {\rm e}^{-m^2 T} \langle W[A]\rangle_x. \qquad (4)$$

Here we also have split off the integral over the loop centers of mass, $x_0^\mu := (1/T)\int_0^T d\tau\, x^\mu(\tau)$, and $\langle(\dots)\rangle_x$ denotes the expectation value of (...) evaluated over an ensemble of x loops; the loops are centered upon a common average position x_0 ("center of mass") and are distributed according to the Gaussian weight $\exp[-\int_0^T d\tau\, \frac{\dot{x}^2}{4}]$.

Crucial for the numerical realization is the observation that substituting $\tau =: Tt$ and introducing *unit loops* y,

$$y(t) := \frac{1}{\sqrt{T}}\, x(Tt), \quad t \in [0,1], \qquad (5)$$

renders the the Gaussian weight independent of the propertime: $\int_0^T d\tau\, \dot{x}^2(\tau)/4 = \int_0^1 dt\, \dot{y}^2(t)/4$ (the dot " $\dot{}$ " denotes always a derivative with respect to the argument). Now, the expectation value of $W[A]$ can be evaluated over the unit-loop ensemble y,

$$\langle W[A(x)]\rangle_x \equiv \langle W[\sqrt{T}A(x_0+\sqrt{T}y)]\rangle_y, \tag{6}$$

where the exterior T-propertime dependence occurs only as a scaling factor of the gauge field and the unit loops in its argument. In other words, while approximating the loop path integral by a finite ensemble of loops, it suffices to have one single unit-loop ensemble at our disposal; we do not have to generate a new loop ensemble whenever we go over to a new value of T.

2.1. *Renormalization*

The effective action is renormalized by adding counterterms to $\Gamma_{\rm eff}$ in order to absorb the strongly cutoff-dependent parts. The counterterms are determined by a set of physical constraints such as the vanishing of $\Gamma_{\rm eff}$ for a vanishing background and the value of the gauge coupling in soft processes at a certain scale. To be specific, we use standard Coleman-Weinberg renormalization conditions for the complete action Γ, containing the bare Maxwell action and the one-loop contribution of Eq. (1),

$$\Gamma[F=0]=0, \quad \left.\frac{\delta\Gamma}{\delta(F^2)}\right|_{F^2/e_{\rm R}^2=\mu^2/2} = \frac{1}{4\,e_{\rm R}^2(\mu)}, \tag{7}$$

where we identify μ with the scale of soft photons measuring the Thomson cross section, i.e., $\mu/m \to 0$. In the examples of Sect. 3, we will only encounter the field strength F which is renormalization group invariant, since it is scaled by the coupling. The substitution $F \to e_{\rm R}F_{\rm R}$ reexpresses the later results in terms of physical coupling and field strength, where $e_{\rm R}$ and $F_{\rm R}$ are the renormalized quantities at the scale μ mentioned above.

From a technical viewpoint, the strongly Λ-dependent terms can be isolated using a heat-kernel expansion of the Wilson loop (which can be performed for arbitrary backgrounds), e.g.,

$$\left\langle W[\sqrt{T}A(x_0+\sqrt{T}y)]\right\rangle_y \;=\; 1 \;-\; \frac{1}{12}T^2\,F_{\mu\nu}[A](x_0)\,F_{\mu\nu}[A](x_0) \;+\; \mathcal{O}(T^4)\,. \tag{8}$$

The counterterms required are in one-to-one correspondence to the terms of the small-T expansion, encoding the short-distance physics; the number of necessary counterterms depends on the dimension of spacetime. While this renormalization program is well under control analytically, the numerical renormalization is complicated by a further problem: evaluating $\langle W\rangle$ with the aid of the loop ensemble does not produce the small-T behavior of Eq. (8) *exactly*, but, of course, only within the numerical accuracy. Unfortunately, even the smallest deviation from Eq. (8) will

lead to huge errors of the effective action, because it induces an artificial singular behavior of the propertime integrand.

Our solution to this problem is to fit the numerical result for $\langle W \rangle$ to a polynomial in T in the vicinity of $T = 0$, employing Eq. (8) as a constraint for the first coefficients. In other words, we insert the analytical information about the short distance behavior of $\langle W \rangle$ for small T explicitly. This fit not only isolates the strongly cutoff-dependent parts which subsequently are subject to the standard renormalization procedure, but also facilitates a more precise estimate of the error bars. Finally, employing this fitting procedure only close to $T = 0$, the infrared behavior ($T \to \infty$) of the integrand remains untouched, and our approach is immediately applicable, also in the case $m = 0$.

2.2. *Numerical simulation*

The numerical computation of the effective action can be summarized by the following recipe:

(1) generate a unit loop ensemble distributed according to the weight $\exp[-\int_0^1 dt \dot{y}^2/4]$, e.g., employing the technique of normal (Gaussian) deviates;
(2) compute the integrand for arbitrary values of T (and x_0); this involves the evaluation of the Wilson loop expectation value for a given background;
(3) perform the renormalization procedure;
(4) integrate over the propertime T in order to obtain the Lagrangian, and also over x_0 for the action.

There are two sources of error which are introduced by reducing the degrees of freedom from an infinite to a finite amount: first, the loop path integral has to be approximated by a finite number of loops; second, the propertime t of each loop has to be discretized. Contrary to this, the spacetime does not require discretization, i.e., the loop ensemble is generated in the continuum.

Approximating $\langle W \rangle$ of Eq. (6) by an average over a finite number N_L of loops, the standard deviation provides an estimate of the statistical error. Approximating the loops by the finite number n_l of space points results in a systematic error that can be estimated by repeating the calculation for several values n_l. The number n_l should be chosen large enough to reduce this systematic error to well below the statistical one. It will turn out that the choice $N_L = 1000$ and $n_l = 100$ for $D = 3$ ($n_l = 200$ for $D = 4$) yields results, for the applications below, which are accurate at the per cent level.

2.3. *Loop Clouds*

Beyond any numerical efficiency, worldline numerics also offers an intuitive approach to effective Lagrangians or functional determinants: Formula (4) together with (6) provides for a descriptive interpretation of the quantum processes. For a given background, the effective-action density receives contributions from all values of the

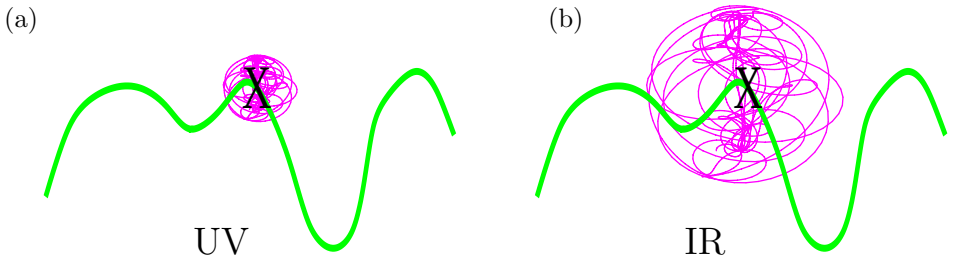

Figure 1: (a/b) small/large-propertime contribution to the effective-action density, picking up small/large-scale information of the background field (UV/IR).

propertime. For instance, for small propertimes, the size of the ensemble of unit loops is also small by virtue of the propertime scaling in Eq. (6), $\sqrt{T}y$. Hence, this *loop cloud* picks up small-scale information about the background field. By contrast, for large propertimes, the loop cloud becomes bloated and receives information about the behavior of the background field over large scales. This zooming in or out of the quantum vacuum is illustrated in Fig. 1.

Analyzing vacuum polarization in a certain background with this concept of loop clouds thereby visualizes the nonlinearities and nonlocalities of the quantum effective action in a vivid way.

3. Examples

3.1. *Constant magnetic background field*

Let us first investigate the efficiency of our numerical loop approach to the scalar functional determinant for a constant magnetic background field B. For this case, the Wilson loop expectation value is exactly known and independent of D:

$$\langle W[A]\rangle = \frac{BT}{\sinh BT}, \quad \text{for} \quad B = \text{const.} \tag{9}$$

Integration over the propertime leads us to the effective-action density, which we plotted in Fig. (2) for $D = 3$ and $D = 4$. The agreement between the exact and the numerical results is satisfactory; the exact results lie well within the error bars, which contain the statistical errors of the Monte-Carlo calculation as well as those of the fitting procedure near $T = 0$ (the latter actually improve the error estimate, since our exact knowledge about the $T = 0$ behavior has been inserted). Our approach is able to cover a wide range of parameter values: in $D = 3$, even the massless limit can be taken without problems. In $D = 4$, the typical logarithmic increase in the strong-field limit with a prefactor proportional to the β function is visible.

3.2. *Step-like magnetic field: quantum diffusion*

As a specific example for a field configuration that cannot be treated in a derivative

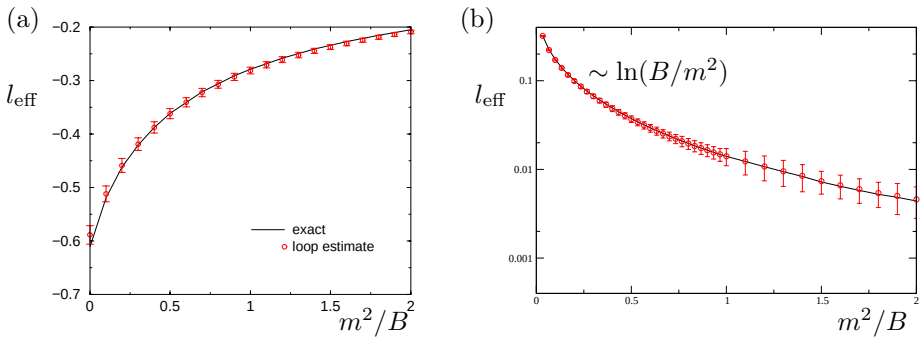

Figure 2: One-loop effective-action density $l_{\rm eff}$ in units of $(B/(4\pi))^{D/2}$ in $D = 3$ (a) and $D = 4$ (b) versus m^2/B for the case of a constant magnetic background field. The analytically known exact results (solid lines) are compared with the numerical findings (circles with error bars).

expansion but inherently involves nonlocal aspects, we consider a time-like constant background field B, resembling a step function in space,

$$B(x,y) \;=\; -\theta(x)\,B\;, \quad \vec{A}(x,y) \;=\; \theta(x)\,\frac{1}{2}\,(y,-x)\,B\;, \tag{10}$$

working for simplicity in $D = 3$. In our approach, discontinuities do not induce (artificial) singularities, but are smoothly controlled by the properties of the loop ensemble. This loop cloud has finite extension and slowly varying density; while running with its center of mass towards and across the step, that part of the volume of the loop cloud which "feels" the magnetic field increases smoothly.

In Fig. 3, we plot our numerical result for the effective-action density across the step (for details, see[6]). As expected, the effective-action density is nonzero even in the region $x < 0$ where the background field $B(\vec{x})$ vanishes. In order to characterize this *quantum diffusion* of the magnetic field further, we fit the effective-action density $\mathcal{L}_{\rm eff}$ in the zero-field region using the ansatz[a]

$$l_{\rm eff} = \frac{(4\pi)^{3/2}\,\mathcal{L}_{\rm eff}}{B^{3/2}} \sim \exp\bigl(-\beta_1\,m\,|x| - \beta_2\,\sqrt{B}\,|x|\bigr). \tag{11}$$

In fact, the numbers $\beta_1 \simeq 3.255$ and $\beta_2 \simeq 0.7627$ fit the data with a high accuracy. The occurrence of two different diffusion lengths $\sim 1/(\beta_1 m)$ and $\sim 1/(\beta_2\sqrt{B})$ may come as a surprise, since one might have expected that the only scale in the field-free region is given by the mass m. However, since the loop cloud is an extended object, it will "feel" the magnetic field even at a large distance; hence, the magnetic field is also a valid scale in the field-free region. This is precisely a consequence of the inherent nonlocality of the quantum processes. Moreover, the diffusion phenomenon appears to be also nonperturbative in the same sense as the Schwinger mechanism

[a]The spacetime coordinates occuring here are, of course, identical to the center-of-mass coordinates x_0 of the worldlines (cf. Sect. 2); we dropped the subscript for simplicity.

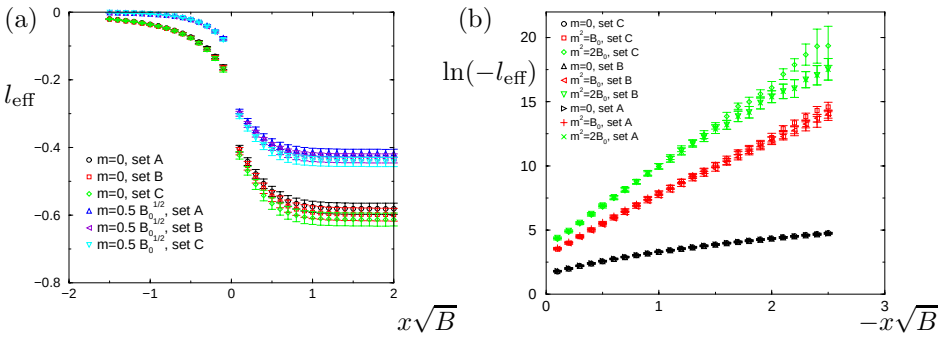

Figure 3: (a) Diffusion profile of the effective-action density in the vicinity of the magnetic step ($x = 0$) in units of $(B/(4\pi))^{3/2}$ for various mass-to-field-strength ratios. (b) A logarithmic plot reveals the exponential nature of the diffusion depth. For a check of the propertime-continuum limit, three different loop ensembles have been used: $n_l = 100$ for set A, $n_l = 75$ for set B, $n_l = 50$ for set C.

of pair production[2]. This is suggested by the functional form Eq. (11), which cannot be expanded in terms of the coupling constant, being rescaled in the field (only an expansion in terms of the square root of the coupling constant is possible).

3.3. *Constant magnetic field at finite temperature*

The presence of a heat bath can be taken into account within the worldline framework by using the imaginary-time formalism: the Euclidean time direction is compactified to a circle with circumference $\beta = 1/\text{temperature}$[10,11].[b] This changes the boundary conditions of the worldline; the loops do not have to close trivially in spacetime, but can now wind around the spacetime cylinder n times:

$$\int\limits_{x(T)=x(0)} \mathcal{D}x \quad \to \quad \sum_{n=-\infty}^{\infty} \int\limits_{\vec{x}(T)=\vec{x}(0),x_0(T)=x_0(0)+n\beta} \mathcal{D}x. \tag{12}$$

Choosing a gauge where the time-like component of the gauge field is time independent, a Poisson resummation of the n-sum disentangles the winding around the cylinder from the trivially closed loops for any background, and the remaining path integral runs over nonwinding loops only. The numerical problem thereby reduces to the zero-temperature case with an additional summation over Matsubara modes, which can be performed to a high numerical accuracy.

Confining ourselves to the constant-magnetic field case, the exact result for the finite-temperature contribution to the Wilson loop EV reads [11,12]

$$\langle W[A]\rangle_x^\beta = 2\sum_{n=1}^{\infty} \frac{TB}{\sinh TB}\, \mathrm{e}^{-\frac{n^2\beta^2}{4T}}. \tag{13}$$

[b] The propertime T should not be confused with the temperature, being characterized by its inverse β in the following.

Concentrating on $D = 3$ scalar QED, we compare the exact results with the numerical estimates in Fig. 4. The propertime integrand (plotted for $m = 1/\beta$, $m^2 = B$) as well as the effective-action density (plotted for $m = 0$) can satisfactorily be reproduced by the numerical approach. The drop-off of the integrand for small propertimes in Fig. 4(a) can be understood in terms of the loop clouds: for small T the loop cloud is simply too small to "see" the compactness of the Euclidean time direction. Furthermore, the Stefan-Boltzmann law for the free energy (= − effective-action density) $\sim \zeta(3)/\beta^3$ is rediscovered in the $B = 0$ limit.

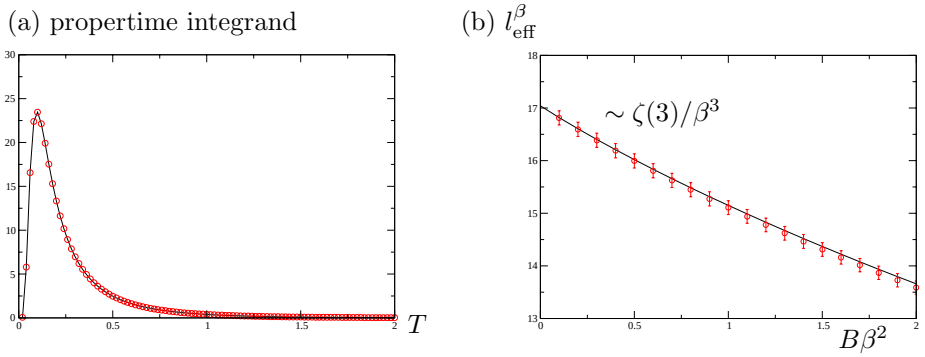

Figure 4: (a) Propertime integrand of the finite-temperature contribution to the effective-action density in $D = 3$ scalar QED ($m = 1/\beta$, $m^2 = B$). (b) Effective-action density contribution at finite temperature in units of $2/(4\pi\beta^2)^{3/2}$ versus $B\beta^2$ in the massless limit.

3.4. *Fermions in the loop*

The worldline formalism allows for an elegant inclusion of fermions by representing the Dirac algebraic elements by path integrals over closed loops in Grassmann space. Unfortunately, this cannot be translated into a numerical algorithm, since the kinetic action for the Grassmann loops is not positive definite; this prohibits a Monte-Carlo algorithm based on importance sampling. Instead, we choose to maintain the Dirac algebraic formulation, which leads to the following representation of the spinor part of Eq. (1):

$$\Gamma^{\rm spinor}_{\rm eff} = -\frac{1}{2}\frac{1}{(4\pi)^{D/2}} \int\limits_{1/\Lambda^2}^{\infty} \frac{dT}{T}\, {\rm e}^{-m^2 T} \left\langle W_{\rm spin}[A] \right\rangle_x , \tag{14}$$

where the "spinorial" Wilson loop is given by

$$W_{\rm spin}[A] = W[A] \times {\rm Tr}\, P_T \, \exp\left(\frac{{\rm i}e}{2} \int_0^T d\tau\, \sigma_{\mu\nu} F^{\mu\nu} \right). \tag{15}$$

Obviously, the spinorial Wilson loop factorizes into the usual one and a trace of a path-ordered exponential of the spin-field coupling. Although this path ordering is

difficult to handle in analytical computations, our numerical algorithm can easily deal with; this is because the path(=loop) is discretized and each point is visited in a path-ordered manner anyway. As a further simplification, the exponential of the spin-field coupling can be projected onto an orthogonal basis of the Dirac algebra (see, e.g., [12]).

Concentrating again on the constant-magnetic-field case, the analytically known result for the spinorial Wilson loop is

$$\left\langle W_{\rm spin}[A]\right\rangle = BT\coth BT \equiv \frac{BT}{\sinh BT}\cosh BT, \tag{16}$$

where the cosh term arises from the trace of the path-ordered exponential in Eq. (15). Comparing the exact result with the numerical one in $D = 3$ as depicted in Fig.5, the agreement in the parameter range $B \lesssim m^2$ is again satisfactory. Only in the strong-field limit does the algorithm become unstable owing to technical reasons: here the exponential increases of the cosh and the sinh function do not cancel numerically as precisely as they should. This technical problem can be solved by first matching the exponential increases of the denominator and the numerator to each other and then performing the division. Whether this matching can be numerically implemented in a background-field independent way has still to be investigated. Beyond this, there are no problems of any fundamental kind limiting the application of the present approach to fermion determinants, in contrast to no-go theorems faced by lattice formulations.

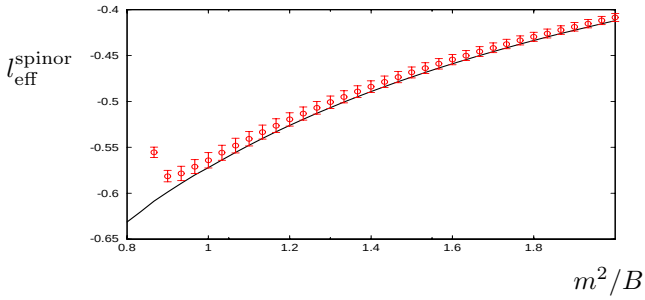

Figure 5: Effective-action density of spinor QED in $D = 3$ for the constant-magnetic-field case (units as in Fig. 2).

4. Conclusion

Our results of the numerical worldline approach to QED effective actions are encouraging: the successful description of the background conditions selected here indicates that the method can be applied to a very general class of backgrounds without the necessity of assuming slow variation, smoothness, or symmetries. In particular, it should be stressed that the algorithm makes no reference to the properties of the background field.

Beyond being an efficient method of computation, our approach also offers a vivid picture of the quantum world: consider a spacetime point x at a propertime T; then, the loop cloud is centered upon this point x with Gaussian "density" and "spread". Increasing or lowering the propertime T corresponds to bloating or scaling down the loop cloud or, alternatively, zooming out of or into the microscopic world. The effective-action density at each point x finally receives contributions from every point of the loop cloud according to its Gaussian weight and averaged over the propertime. This gives rise to the inherent nonlocality and nonlinearity of the effective action, because every point x is influenced by the field of any other point in spacetime experienced by the loop cloud.

We would like to conclude with some further remarks and caveats. Of course, the Monte-Carlo procedure requires that the loops are distributed in Euclidean spacetime in order to guarantee the positivity of the action. This can lead to difficulties (also shared by many other approaches) when the method is applied to the computation of Greens functions with Minkowskian momenta. However, this does not pose a problem for the inclusion of Minkowskian electric fields which can simply be taken into account by an imaginary Euclidean field strength. For instance, pair production in inhomogeneous electric fields can be studied in this way. Finally, the analogy between worldline path integrals and Brownian motion implies that the loops in our loop cloud should have Hausdorff dimension 2; on a computer, this can, of course, never be realized. However, we expect that this may lead to sizeable errors only in the extreme case of a massless or very light particle in the loop *and* a background field with fluctuations on all scales; only then are the large-propertime contributions not suppressed, and the coarse structure of the large loop clouds are insensitive to small-scale fluctuations. This failure will manifest itself in the practical impossibility of performing the propertime-continuum limit. On the other hand, if the continuum limit can be taken, the loops will be sufficiently close to Hausdorff dimension 2.

Acknowledgements

H.G. would like to thank M. Bordag for organizing this productive workshop and acknowledges discussions with W. Dittrich, G.V. Dunne, R.L. Jaffe, G.-L. Lin, C. Schubert, M. Reuter, and H. Weigel. H.G. is grateful for the warm hospitality of the IFAE at Barcelona Autonoma U., where this manuscript was completed. This work was supported by the DFG under contract Gi 328/1-1.

References

1. W. Heisenberg and H. Euler, Z. Phys. **98**, 714 (1936);
   V. Weisskopf, K. Dan. Vidensk. Selsk. Mat. Fy. Medd. **14**, 1 (1936).
2. J. S. Schwinger, Phys. Rev. **82**, 664 (1951).
3. V. P. Gusynin and I. A. Shovkovy, J. Math. Phys. **40**, 5406 (1999).
4. D. Cangemi, E. D'Hoker and G. Dunne, Phys. Rev. **D 52**, 3163 (1995); Phys. Lett. **B419**, 322 (1998).
5. M. Bordag and K. Kirsten, Phys. Rev. D **60**, 105019 (1999);
   P. Pasipoularides, Phys. Rev. D **64**, 105011 (2001).
6. H. Gies and K. Langfeld, Nucl. Phys. B **613**, 353 (2001).
7. Z. Bern and D.A. Kosower, Nucl. Phys. **B362**, 389 (1991); **B379**, 451 (1992);
   M.J. Strassler, Nucl. Phys. **B385**, 145 (1992).
8. M. G. Schmidt and C. Schubert, Phys. Lett. **B318**, 438 (1993);
   R. Shaisultanov, Phys. Lett. **B378**, 354 (1996);
   M. Reuter, M. G. Schmidt and C. Schubert, Ann. Phys. **259**, 313 (1997).
9. C. Schubert, hep-th/0101036, to appear in Phys. Rep. (2001).
10. D. G. McKeon and A. Rebhan, Phys. Rev. **D 47**, 5487 (1993);
    I. A. Shovkovy, Phys. Lett. **B441**, 313 (1998).
11. H. Gies, Phys. Rev. D **60**, 105002 (1999).
12. W. Dittrich and H. Gies, Springer Tracts Mod. Phys. **166**, 1 (2000).